Minimal change in Antarctic Circumpolar Current flow speeds between Glacial and Holocene

I.N. McCave[1]*, S.J. Crowhurst[1], G. Kuhn[2], C-D. Hillenbrand[3] and M.P. Meredith[3 & 4]

[1]Godwin Laboratory for Palaeoclimate Research, Department of Earth Sciences, University of Cambridge, Downing Street, Cambridge, CB2 3EQ, U.K.

[2] Alfred-Wegener-Institut Helmholtz-Zentrum für Polar- und Meeresforschung, Am Alten Hafen 26, D-27568 Bremerhaven, Germany.

[3]British Antarctic Survey, High Cross, Madingley Road, Cambridge CB3 0ET, U.K.

[4] Scottish Association for Marine Science, Oban, U.K.

* Correspondence to INMcC at e-mail: mccave@esc.cam.ac.uk

The Antarctic Circumpolar Current is the major westerly wind- and buoyancy-driven current that encircles the globe, connecting all oceans at ~45° to 70°S[1,2,3]. It plays a key role in mixing and ventilating the oceans[4,5] and is the site of primary productivity that helps regulate global atmospheric CO_2 levels[6]. It has been maintained that during the last glacial maximum the current's flow was either faster[7] than present or unchanged[8] under stronger[9] or weaker[10] winds and that the whole current shifted to the north[11], or not[8]. Here we compare last glacial maximum to Holocene difference of bottom speeds through the Drake Passage/Scotia Sea flow constriction and show essentially no change in the *average* flow through the region, at least in terms of its barotropic component. However, flow at the last glacial maximum was significantly slower in the southern ice-covered portion of the area[12] (south of 56° S), and (non-significantly) faster in the north, which implicates shielding from wind stress by perennial sea-ice in the southern part of the current. These inferences are based on Holocene and last glacial maximum averages of the Sortable Silt mean grain size[13] for 12 cores across the Scotia Sea. Because momentum imparted at the surface is balanced at depth by topographic form drag, relative invariance of the bottom speeds argues against substantial changes in wind stress. Slower flow over rough topography in the south implies reduced diapycnal mixing in this key region, consistent with reduction in this component of the overturning circulation[4].

The strength of the Antarctic Circumpolar Current (ACC) is controlled by the integrated wind stress across the whole circumpolar belt[14,15], and buoyancy forcing comprising heat and fresh water inputs[3,5]. Because the ACC is zonally unbounded, without continental barriers against which zonal pressure gradients can be established to retard the flow, the primary balance is between forcings applied at the surface and topographic interactions at the seabed (in

particular form drag, requiring non-zero bottom velocities). Downward momentum flux via interfacial form stress is balanced at the seabed by form drag[16], with mesoscale eddies being inherently involved in this vertical transfer. Current speeds may be up to a few tens of cm s^{-1} at the seabed, but they are generally intensified near the surface, and around most of its path the ACC is observed to have an equivalent barotropic structure[17] (i.e. current shear is aligned with the mean flow). However, bottom currents alone are not sufficient to infer the full vertical structure of the transport.

The strong eddy field in the ACC helps determine its three-dimensional circulation. Theoretical arguments indicate that under increasing energy input from strengthening winds the ACC would not increase its mean transport, but instead the eddy field would be energised[18]: this was dubbed "eddy saturation". Recent tests with observational data and models show that ACC transport varies very little in response to changes in winds on interannual timescales, but the eddy field varies much more[19], indicating that the ACC is close to eddy saturation. The adjustment timescale for changing the density structure across the ACC is long (decades or longer) due to the required adjustment of the ocean pycnocline to the north: this also limits variation in ACC transport on shorter timescales[20]. Mesoscale eddies associated with the ACC extend to the seabed[16,21], and also influence the overturning circulation in the Southern Ocean[22,23]. Increases in the directly wind-driven component of the overturning (northward Ekman transport) can act to increase baroclinic instability and generate more eddies, which reduce isopycnal steepness and compensate some of the acceleration in overturning[22]. However, changes in wind and buoyancy forcing can still exert significant changes in the strength of overturning and hence the gas exchange rate with the atmosphere[5,23]. Changes in both wind strength and position can affect the level of coupling with the ocean jets and hence impact on the

flow. The frontal system in the ACC at the last glacial maximum **(**LGM) has been suggested to have shifted to the north[11,24] (the predominant view), or remained at the same latitude as at present[8], and the ACC to have flowed faster than present at the LGM[7,24]. Numerical models have managed to reproduce all these scenarios[10].

CO_2 drawdown at the LGM was controlled by several factors, some of which were wind-related, including upwelling of nutrients[5,24], fertilisation by iron-bearing dust[9] and coverage by sea-ice, all affecting productivity[6,11]. In addition, the Southern Ocean was more stratified at the LGM due to colder deep-water temperatures and fresher surface waters[5]. Whether the dust flux was mainly wind-speed controlled is unresolved[26].

The whole ACC and its fronts pass through the Drake Passage and Scotia Sea, making it a convenient choke point to monitor flow speeds, fluxes and hydrography[15]. Because of the potential space-time aliassing problem caused by moving ACC fronts (i.e. a temporal change recorded in a sediment core might reflect a latitudinal shift in the current axis rather than an overall change in ACC flux), our strategy has been to examine the ACC in the Scotia Sea where flow is forced to pass through an 800 km-wide gap between the North and South Scotia Ridges. Even here limited frontal movement may have occurred, so a large number of cores (12) was studied, with the distance between cores along the transect (Fig. 1) being 95 km on average but not exceeding 150 km. A minimum of ten samples from each of the Holocene and LGM *sensu lato* (Supplementary Information) sections in each core (dated by correlation of downcore magnetic susceptibility to the EPICA ice core dust record[27]) were analysed to generate averages for the two climatic extremes (see Methods). Holocene and LGM averages of the Sortable Silt mean size ($\overline{SS}$, the mean size of the 10-63 μm terrigenous sediment fraction) proxy for bottom

86 current flow speed[13] were measured for each core. Numerous studies have shown this parameter
87 to record relative flow speed (a size change of 1 μm equates to flow speed differences of ~2 to 3
88 cm/s at $\overline{SS}$ = 22 to 14 μm mean size), and to be tightly linked to climatic and oceanographic
89 variations[13] (Supplementary Information). The particle size responds to scalar speed and records
90 mean plus eddy-related components of near-bed flow speed.
91
92 The Scotia Sea is a key gateway for the ACC, whose flux could potentially have been
93 greater at the LGM through the exit at the North Scotia Ridge[28]. Frontal positions have recently
94 been mapped via satellite radar altimetry[29] (Fig. 1). Analysis of 10 years of such data shows
95 variable frontal locations[29] which are likely to be even more variable on the 10^4-year term that
96 our averages represent, so that it is difficult to relate sediment properties to a narrow frontal
97 position. Most of the core locations are, and presumably were, affected by a frontal zone for
98 some of the time. A snapshot of measured flow speeds shows sharply defined flow bands
99 (Supplementary Fig. S5), but these zones would appear broader in averaged sediment records.
100
101 Referring to the grain-size proxy as 'flow speed'[13], it is clear that (i) flow speed increases
102 to the North during both the LGM and the Holocene (Fig. 2), matching the modern trend in
103 speed measured by acoustic Doppler profiler (Supplementary Fig. S5), inferred from
104 geostrophy[15], and recorded in overall sediment texture[25], and (ii) this meridional gradient in
105 zonal flow speed was steeper at the LGM. In five cores there is a significant ($P < 0.01$) difference
106 between LGM and Holocene (Fig. 2). However there is no significant difference between the two
107 periods averaged across all cores, the difference being only 0.28 μm (not significant as $P > 0.2$)
108 (Supplementary Table T2). This indicates that overall the ACC bottom currents in the Scotia Sea
109 were not significantly faster at the LGM. The north and south of the area differ in that four of the

five cores north of ~56° S (beyond 650 km in the transect displayed in Fig. 2) show slightly stronger (but not statistically significant) LGM flow whereas to the south of 56°S six of seven cores show weaker LGM flows, of which three indicate significantly weaker flow ($P < 0.01$). In an earlier study, in which the authors concluded faster overall flow speed at the LGM, a possible influence of changing contents of biogenic particles on the observed grain-size changes was not excluded[25]. The northern boundary of slower LGM speeds in our data corresponds closely to the maximum northern extent of LGM summer sea-ice[12], i.e. the southern half of the area was permanently ice covered. At the southernmost end of the transect three cores show essentially no difference.

Perennial sea-ice cover will impact on ocean current speeds by changing the transmission of wind stress to the ocean. Diatom populations have been used to show that the summer sea ice limit was at ~56°S (Fig.1) over the period 30-22 ka[12] (and Supplementary Information), though may have moved poleward during the later LGM (22-19 ka). South of this latitude, if the ice cover at the LGM were relatively immobile, the slower current speeds we have deduced here could be attributed to the cover diminishing the effect of wind stress on the ocean. Under these circumstances, it is not possible to determine the extent to which winds differed from those in the Holocene. North of this zone, whilst changes in seasonal sea ice extent and mobility are complicating factors, the insignificantly-changed bottom speeds between the LGM and Holocene argue against dramatic changes in wind stress. The very southernmost area (cores 10-12) show no change, indicative that it is comparably affected by LGM and Holocene ice cover. Taken as a whole, the differences recorded across the Scotia Sea strongly suggest that the wind effect on bottom flow speeds is significantly modulated by sea-ice cover.

In addition to the important eddy-induced isopycnal mixing contribution to Southern Ocean overturning, diapycnal mixing due to strong bottom flows over rough topography in the Scotia Sea, leading to high benthic and interior mixing, is also important[4]. Slower LGM flow in the southern part of this mixing 'hot spot' suggests that this diapycnal contribution to the Southern Ocean overturning may have been reduced. Thus the stronger modern/Holocene than LGM bottom currents in the southern part of the area could have exerted indirect impact on the overturning circulation and hence climate. Similar glacial and Holocene bottom currents in the north would also be consistent with similar ACC barotropic flow, possibly because the forcings themselves had not changed greatly. The timescale for adjustment of the ACC is short compared to the time interval of the sediment-derived data, thus adjustment of pycnocline north of the ACC is presumed not to be a restriction[20]. Eddy saturation could limit the ACC transport in a stronger-wind scenario, yielding insignificantly changed bottom velocities, but it should be noted that the sediment-inferred data used here relate to scalar mean speeds, and so will include the eddy component of the velocity. The fact that a non-significant change is seen in the seasonally ice-covered part of the area (north of 56° S) may thus also be interpreted as relatively little change in atmospheric forcing of the ACC (including its eddy field). We note that this argument relies on the vertical structure of the ACC being relatively invariant on long timescales, which cannot be proved from bottom current speeds alone. Nonetheless, inference of relative invariance in the wind forcing derives also from the equilibrium balance of the ACC, where momentum imparted at the surface is balanced by form drag created by bottom currents setting up pressure gradients across bathymetric features[16].

If LGM wind stress were similar to present, the high glacial dust flux seen in Antarctic ice cores, often used as a basis for inferring stronger winds, must be mainly ascribed to other

158 environmental changes in source areas including an exposed Patagonian continental shelf, lack
159 of vegetation, dryer soil and high glacial outwash sediment supply[26]. If the present data are
160 regarded as inserting a peg in the speculative range, then the LGM models with northward
161 frontal shifts, reduced deep mixing under ice, and relatively invariant ACC flow should be
162 favoured.

163

164 Methods

165 **Cores:** Twelve cores forming the transect across the Scotia Sea were identified in the collections
166 of the British Antarctic Survey (BAS) and the Alfred Wegner Institute (AWI) (Fig. 1). The
167 recovered sediments consist of terrigenous mud, and muds with variable amounts of diatoms but
168 very little carbonate[25,27]. Given the distribution of sediments in the Scotia Sea, our network of
169 cores captures the flow field as well as possible.

170 **Age Models:** Magnetic susceptibility records of the cores were correlated to the EPICA Dome C
171 (EDC) ice core dust records to provide ice core equivalent ages on the EDC3 scale[27]. This has
172 been established as consistent with chronological constraints from AMS ^{14}C dating of organic
173 matter and biostratigraphy. The age limits for the LGM *sensu lato* (18 ka to base of Marine
174 Isotope Stage 2 at 28 ka) were chosen based on the uniform deuterium record from the EDC ice
175 core over this period (Supplementary Fig. S1). A minimum of ten samples from each of the
176 Holocene (0-12 ka) and LGM sections in each core were analysed to generate averages for the
177 two climatic extremes, averaged over their 12 and 10 ka duration respectively. Samples are thus
178 ~ 1000 years apart (Supplementary Table T3).

Sediment processing: Carbonate and opaline silica were removed from the <63 μm grainsize (mud) fraction. Grainsize analysis of the resulting terrigenous fine fraction was by Coulter Counter (Multisizer-3). Holocene and LGM averages of the Sortable Silt mean size ($\overline{SS}$, the mean size of the 10-63 μm fraction) proxy for flow speed[13] were calculated for each core. Significance of the difference between means was assessed by a 2-tailed t-test where greater than 99% ($P<0.01$) was considered significant.

Data: The data reported here are tabulated in the Supplementary Information and are archived at the PANGAEA database, doi:

Correspondence and requests for materials should be addressed to INMcC.

Acknowledgements

This work was funded by the award of an Emeritus Fellowship to INMcC by the Leverhulme Foundation. We are grateful to Dr Robert Pugh for his Coulter Counter measurements on core PC287 and Dr. Carol Pudsey for providing some of the magnetic susceptibility data on the BAS cores. We are grateful for discussions with Andy Watson, Harry Bryden, Agatha de Boer and Alberto Naveira-Garabato.

Author contributions

The study was conceived by INMcC who performed the age modelling, made some of the size measurements and wrote the paper. SJC prepared samples and made some of the size measurements. GK (who had support from the ESF HOLOCLIP project) and C-DH provided some prepared samples and ancillary core data that enabled age modelling, and provided critical

input on regional oceanography and sedimentation. MPM provided input and writing on the physical oceanographic interpretation of the sediment records. All authors contributed to the final version.

Additional information

Supplementary information is available in the online version of the paper.

Reprints and permissions information is available online at www.nature.com/reprints.

Competing financial interests

The authors declare no competing financial interests

References

1. Rintoul, S. R., Hughes, C.W. and Olbers, D., The Antarctic Circumpolar Current System. *In:* Ocean Circulation and Climate. (eds.) G. Siedler, J. Church and J. Gould: 271-302.Academic Press, New York (2001)
2. Tansley C.E. & Marshall D.P., On the dynamics of wind-driven circumpolar currents. *J. Phys. Oceanogr*: **31**, 3258-3273 (2001)
3. Hogg, A.M., An Antarctic Circumpolar Current driven by surface buoyancy forcing. *Geophys. Res. Lett*. **37**, L23601 (2010)
4. Watson, A.J., et al. Rapid cross-density ocean mixing at mid depths in Drake Passage measured by tracer release. Nature, **501**, 408-413 (2013)
5. Watson, A.J. & Naveira Garabato, A.C., The role of Southern Ocean mixing and upwelling in glacial-interglacial atmospheric CO_2 change. *Tellus*, Ser. **B 58**, 73–87 (2006)
6. Frank, M. *et al.*, Similar glacial and interglacial export bioproductivity in the Atlantic sector of the Southern Ocean: multiproxy evidence and implications for glacial atmospheric CO_2. *Paleoceanography* **15**, 642–658 (2000)

7. Mazaud, A., Michel, E., Dewilde, F. & Turon, J.L., Variations of the Antarctic Circumpolar Current intensity during the past 500 ka. *Geochem. Geophys. Geosyst.* **11**, Q08007 (2010)
8. Matsumoto, K., Lynch-Stieglitz, J. & Anderson, R.F., Similar glacial and Holocene Southern Ocean hydrography. *Paleoceanography* **16**, 445–454 (2001)
9. Martinez-Garcia, A. et al., Links between iron supply, marine productivity, sea-surface temperature, and CO_2 over the last 1.1 Ma. *Paleoceanography* **24**, PA1207 (2009)
10. Rojas, M. et al., The southern westerlies during the last glacial maximum in PMIP2 simulations. *Clim. Dynam*. **32**, 525-548 (2005)
11. Gersonde, R., Crosta, X., Abelmann, A. & Armand, L., Sea-surface temperature and sea ice distribution of the Southern Ocean at the EPILOG Last Glacial Maximum - a circum-Antarctic view based on siliceous microfossil records. *Quat. Sci. Rev*. **24**, 869–896 (2005)
12. Collins, L.G., Pike, J., Allen, C.S. & Hodgson, D.A., High-resolution reconstruction of southwest Atlantic sea-ice and its role in the carbon cycle during marine isotope stages 3 and 2. *Paleoceanography* **27**, PA3217 (2012)
13. McCave, I.N. & Hall, I.R., Size sorting in marine muds: Processes, pitfalls and prospects for palaeoflow-speed proxies. *Geochem. Geophys. Geosyst*. **7**, Q10N05, 37 pp, (2006).
14. Allison, L. C., Johnson, H.L. Marshall, D.P. & Munday, D.R. Where do winds drive the Antarctic Circumpolar Current? *Geophys. Res. Lett*. **37**, L12605 (2010)
15. Meredith, M.P. et al., Sustained monitoring of the Southern Ocean at Drake Passage: past achievements and future priorities. *Rev. Geophys.* **49**, RG4005 (2011)
16. Johnson, G. C. & Bryden, H.L., On the size of the Antarctic Circumpolar Current. *Deep-Sea Res.* **36**, 39–53 (1989)
17. Killworth, P., An equivalent-barotropic mode in the fine resolution Antarctic model. *J. Phys. Oceanogr*. **22**, 1379–1387 (1992)
18. Straub, D. N., On the transport and angular momentum balance of channel models of the Antarctic Circumpolar Current. *J. Phys. Oceanogr.* **23**, 776–782 (1993)
19. Meredith, M. P., Woodworth, P.L. Hughes, C.W. & Stepanov, V. Changes in ocean transport through Drake Passage during the 1980s and 1990s, forced by changes in the Southern Annular Mode. *Geophys. Res. Lett.* **31**, L21305 (2004)

20. Allison, L. C., Johnson, H.L. & Marshall, D.P., Spin-up and adjustment of the Antarctic Circumpolar Current and global pycnocline. *J. Mar. Res.* **69**, 167-189 (2011)
21. Nikurashin, M., Vallis, G.K. & Adcroft, A., Routes to energy dissipation for geostrophic flows in the Southern Ocean. *Nature Geoscience* 6,48–51(2013), doi:10.1038/ngeo1657
22. Marshall, J. & Speer, K. Closure of the meridional overturning circulation through Southern Ocean upwelling. *Nature Geosci*. 5, 171–180 (2012)
23. Meredith, M.P., Naveira Garabato, A.C., Hogg, A.M. & Farneti, R., Sensitivity of the overturning circulation in the Southern Ocean to decadal changes in wind forcing. *J. Clim.* **25**, 99-110 (2012)
24. Toggweiler, J.R., Russell, J.L. & Carson, S.R., Midlatitude westerlies, atmospheric CO_2, and climate change during the ice ages. *Paleoceanography* **21**, PA2005 (2006).
25. Pudsey, C.J., & Howe, J.A., Quaternary history of the Antarctic Circumpolar Current: evidence from the Scotia Sea. *Mar. Geol.* **148**, 83-112 (1998).
26. Sugden, D.E., McCulloch, R.D., Bory, A.J-M. & Hein, A.S., Influence of Patagonian glaciers on Antarctic dust deposition during the last glacial period. *Nature Geoscience* **2**, 281-284 (2009).
27. Pugh, R.S., McCave, I.N., Hillenbrand, C.D. & Kuhn, G., Circum-Antarctic age modelling of Quaternary marine cores under the Antarctic Circumpolar Current: Ice-core dust–magnetic correlation. *Earth Planet. Sci. Lett.* **209**, 113-123 (2009).
28. Smith, I.J., Stevens, D.P., Heywood, K.J. & Meredith, M.P., The flow of the Antarctic Circumpolar Current over the North Scotia Ridge. *Deep-Sea Res. I.* **57**, 14–28 (2010).
29. Sokolov, S. & Rintoul, S.R., Circulation structure and distribution of the Antarctic Circumpolar Current fronts: 1. Mean circumpolar paths. *J. Geophys. Res*. **114**, C11019 (2009).

Ito, T. & Marshall, J., Control of lower-limb overturning circulation in the Southern Ocean by diapycnal mixing and mesoscale eddy transfer. *J. Phys. Oceanogr*., **38**, 2832–2845 (2008)

Figure Captions.

Fig. 1.

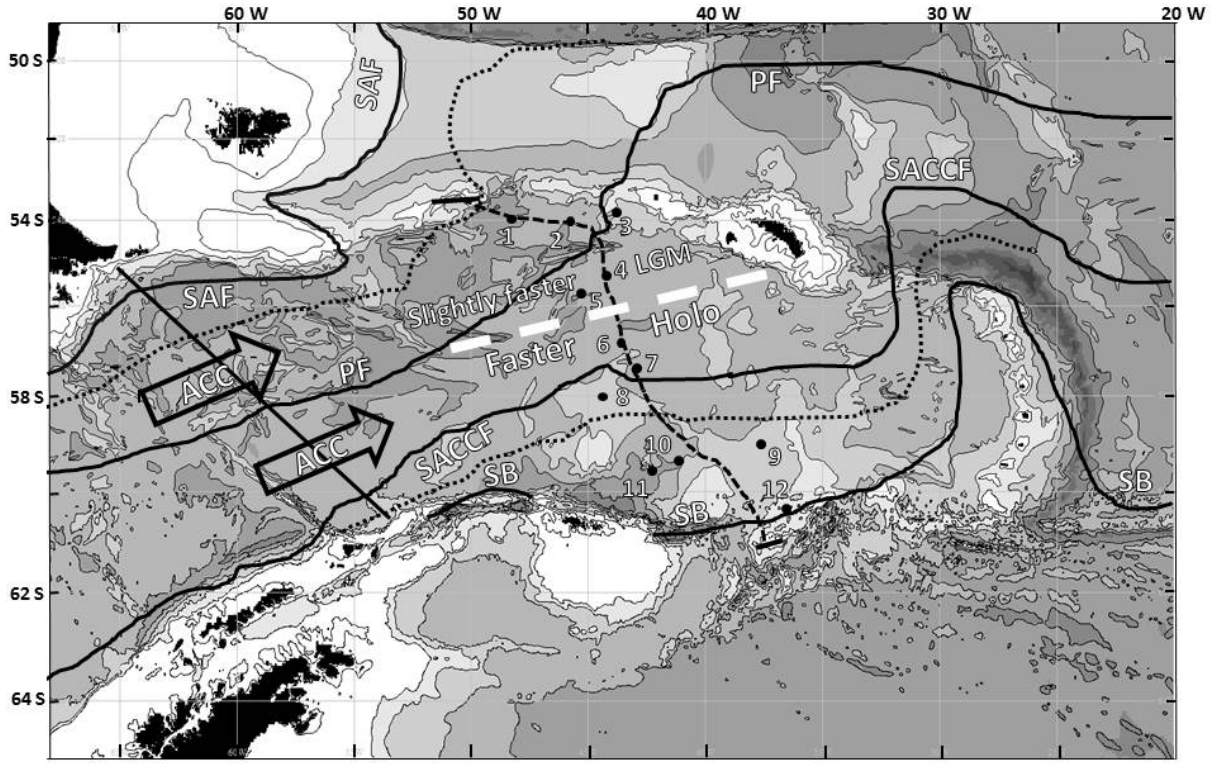

290

291 Scotia Sea core locations.

292 Contours at 0.2,1,2,3,4,5 km on GEBCO basemap. Solid contours mark Fronts: SubAntarctic

293 (SAF); Polar (PF); Southern ACC (SACCF); Southern Boundary (SB): dotted lines mark

294 subsidiary frontal positions[29]. Straight line marks Drake Passage current speed transect

295 (Supplementary Fig. 5); wavy dashed line is projection line for the cores shown in Figure 2.

296 White dashed line between cores 5 and 6 separates the southern faster Holocene flow region

297 from the north, and is the location of the summer sea-ice (SSI) boundary at 29-22 ka[12]

298 (Supplementary Information). Core details are given in Supplementary Table T1.

299

300 **Fig. 2.**

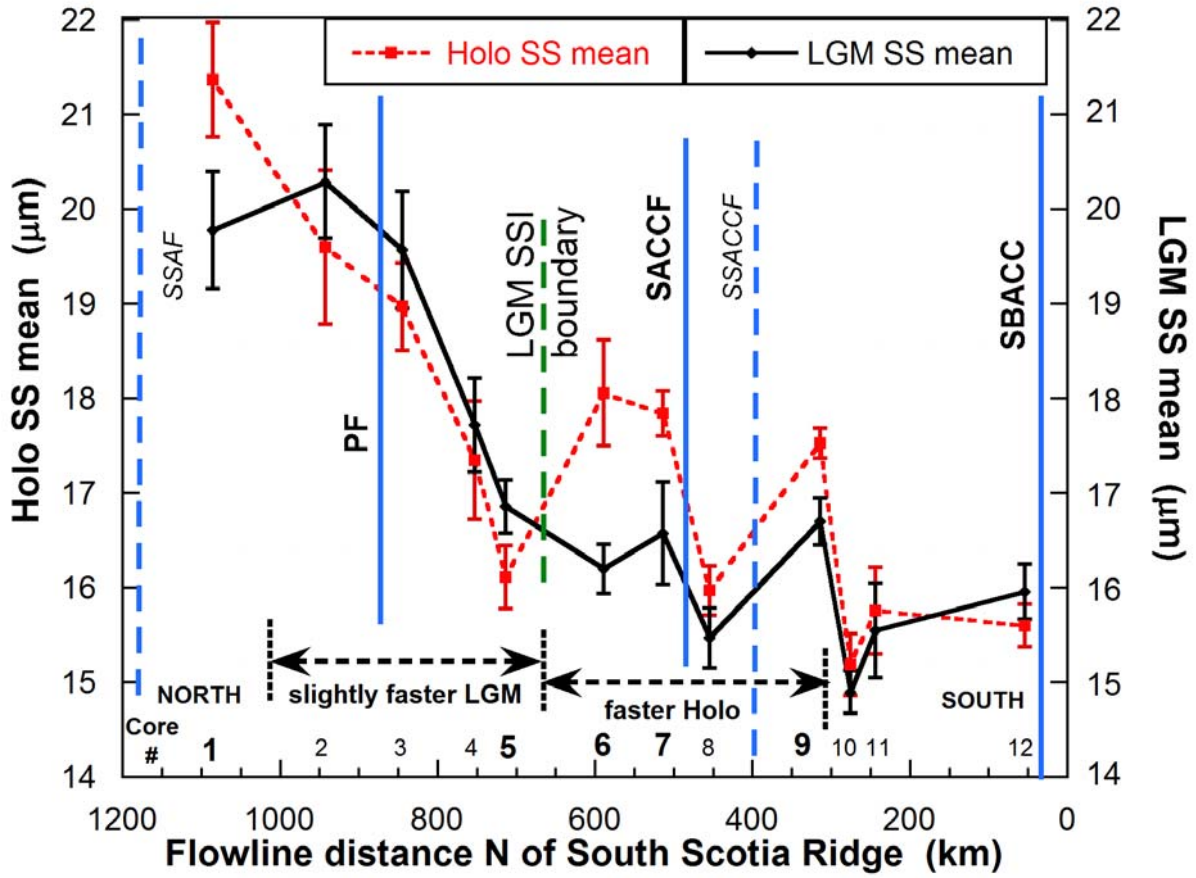

301

302 Average Sortable Silt ($\overline{SS}$) particle size.

303 $\overline{SS}$ averaged for the LGM and Holocene (see Methods). Error bars are ±2 s.e.m (analytical error
304 of ±0.5 μm is not propagated). The x-axis is distance along the projection line on Fig. 1. Bold
305 core numbers indicate significant (P<0.01) LGM-Holocene differences (Supplementary Table
306 T2). Modern frontal positions (and subsidiaries *SSAF* and *SSACCF*) are indicated[29] (acronyms in
307 Fig. 1). South of 56°S LGM flow was significantly slower than Holocene flow (cores 6-9), while
308 cores 10-12 show no significant change. North of 56°S (cores 2-5) flow during the LGM was
309 faster than further south, with a non-significant decrease in the Holocene.